Development of an HPFRC for Use in Flat Slabs

Julia Blazy, Sandra Nunes(✉), Carlos Sousa, and Mário Pimentel

CONSTRUCT-LABEST, Department of Civil Engineering,
Faculty of Engineering, University of Porto, Porto, Portugal
snunes@fe.up.pt

Abstract. Fibre-reinforced cementitious materials represent one of the most significant developments in the field of concrete technology of the last decades. The improved performance of this new class of materials (in terms of workability, compressive strength, flexural/tensile behaviour and/or durability) allows rethinking several of the existing structural solutions. This paper describes research on high-performance fibre reinforced concrete (HPFRC) to be used at the slab-column connection zones of flat slabs, in order to improve its punching shear resistance. Design of Experiments (DoE) approach was used to design HPFRC paste and aggregate particle phases. As such, a central composite design was carried out to mathematically model the influence of mixture parameters and their coupled effects on deformability, viscosity and compressive strength. After that, a numerical optimization technique was applied to the derived models to select the best mixture, which simultaneously, maximizes aggregates content and allows achieving a compressive strength of 90–120 MPa, while maintaining self-compactability (SF1 + VS2), incorporating 1% steel fibres content.

Keywords: High-Performance Fibre Reinforced Concrete (HPFRC) · Mix-design · Self-compacting · Flexural behaviour · Steel fibres

1 Introduction

During the last three decades, concrete has emerged from a rather simple mass construction material towards a high-performance material, which can be tailored for specific applications and according to user specifications. The rapid evolvement in terms of enhanced workability (self-compacting ability) and compressive strength was made possible by the development of superplasticizers and mix-design methods. At increasing strength, concrete becomes more brittle, which can be compensated for by the incorporation of fibres. The fibres can increase the ductility in compression as the fibres transfer stress during cracking. Figure 1 maps the most common fibre-reinforced cementitious composites with regard to compressive strength and fibre content, namely, engineered cementitious composites (ECC), ultra-high fibre performance fibre reinforced composites (UHPFRC), high-performance fibre reinforced concrete (HPFRC) and traditional fibre reinforced concrete (FRC).

The potential for an increase in compressive strength due to an increase in fibre content is less significant compared to the tensile strength [1, 12]. Fibres can improve

P. Serna et al. (Eds.): BEFIB 2020, RILEM Bookseries 30, pp. 209–220, 2021.
https://doi.org/10.1007/978-3-030-58482-5_19

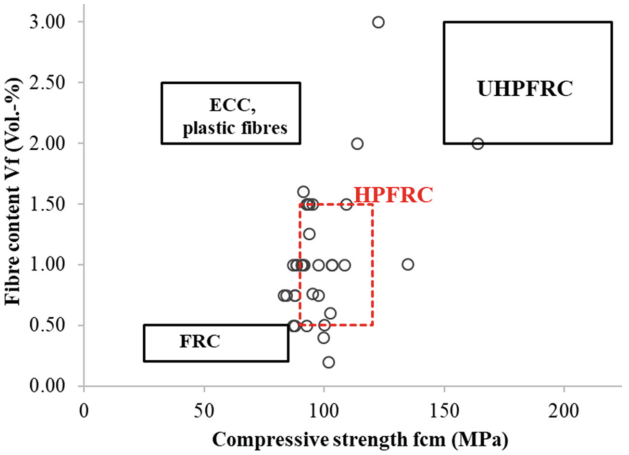

Fig. 1. Most common range of different fibre-reinforced cementitious composites, concerning compressive strength and fibre content

the tensile and flexural behaviour of FRC; its effect depends on the content, fibre type, fibre orientation and distribution, and matrix strength [1]. The use of steel fibre hybridisation has also been found to enhance the pre- and post- cracking response of FRC [2]. The performance of FRC in tension usually improves at increasing fibre content; but beyond a threshold value, the performance might even decrease due to the loss of workability and entangling of interacting fibres during pull-out (lower efficiency of the fibres). The effect of coarser aggregates in this context is also crucial concerning the performance in both the fresh and the hardened states. The addition of fibres in concrete affects its characteristics in the fresh state due to the larger surface area of fibres, which requires more paste to envelop and lubricate the fibres [12]. In particular, stiff fibres decrease the packing density of the aggregates; this effect is more pronounced the larger the aggregates are, compared to the fibre length [12]. In most cases, the FRC mix-design is a trade-off between workability requirements, desired post-cracking behaviour and economical aspects. Since fibres increase the material costs, optimum fibre content has to be determined.

The current study deals with the materials selection, formulation and optimization of an HPFRC mixture to be used in a localised area at the slab-column connection zones of flat slabs (the rest of the slab being cast with normal-strength concrete), in order to improve its punching shear resistance. The strategy followed in this study was to optimize the two main parts of the composite separately. Firstly, optimise the paste phase and the aggregate particle phase to achieve a target compressive strength of 90–120 MPa and self-compacting ability. A fixed fibre content and a single fibre type were used at this stage. Secondly, combining the optimized concrete with a hybrid fibres mixture (new hooked-ends macro steel fibres + straight micro steel fibres) and assess its influence on flexural behaviour, in order to find the best combination. The current paper reports only on the first part of the study.

Some literature studies on HPFRC with compressive strengths close to the target range of 90–120 MPa are reported in Table 1. Regarding the performance in the fresh

state, these include conventional vibrated concretes (slump: 17.5 and 13.0 cm [6]) as well as self-compacting concretes (slump flow: 71–78 cm [2]; 76 cm [7]; 65–75 cm [11]). Compressive strength and fibre content data from these studies are also plotted in Fig. 1, identifying the zone where most HPFRC mixtures can be found. It can be observed that in most HPFRCs the fibre content ranges from 0.5% to 1.5%.

Table 1. Characteristics of several HPFRC materials from different studies.

Ref.	Binder	w/b	dmax (mm)	V_f	lf/df; geometry	fcm,28d (MPa)
[1]	ASTM Type I cement	0.25 (w/c)	10	0.5%; 1%; 1.5%	40/0.62; 1HE	88; 90; 93
				0.5%; 1%; 1.5%	50/0.62; 1HE	87; 91; 93
				0.5%; 1%; 1.5%	60/0.75; 1HE	87; 92; 94
[2]	CEM I 52.5R	0.27 (w/c)	10[a]	0.75%+0%	60/0.9; 1HE+13/0.20; S	88
				0.562%+0.188%		84
				0.375%+ 0.375%		83
				0.188%+0.562%		88
				0%+0.75%		98
				1.0%+0%	60/0.9; 2HE+13/0.20; S	89
				0.75%+0.25%		89
				0.5%+0.5%		87
				0.25%+0.75%		91
				0%+1.0%		98
[3]	PC+SF+FA	0.25	13	1.25%	30/0.50; 1HE	94
[4]	Cement CPN50	0.30 (w/c)	10	0.76%	-; -	95
[5]	PC 42.5 Type I+ SF	0.24 (w/c)	12.5[b]	0.2%	28/0.40; 1HE	102
				0.4%		100
				0.6%		102
				1.0%		103
[6]	OPC+SF	0.295	10[c]	1%	13/0.18; S	103
				2%		114
[7]	CEM+mS+LP	0.24	10[b]	0.5%	30/0.55; C	100
[8]	OPC+zSF+FA	0.195	10[d]	0.50%	30/0.50; 1HE	93
				1%		108
[9]	PC Type II+LP	0.40 (w/c)	12.7	1.6%	36/0.70; 1HE	91
[10]	CEM II/B-M (S-V) 42.5 N+ SF	0.20	11[e]	1%+0.5%	13/0.20+30/0.60	109
		0.18	8[e]	3% (total)	13/0.20+30/0.60+50/0.1	122
		0.18	11[e]	0.5%+0.5%+0.5%	13/0.20+30/0.60+50/0.1	95
[11]	CEM I 42.5R HSR LA+SF	0.32 (w/c)	8[e]	0.7%+0.3%	6/- + 30/-	130-140
[12]	CEM I 52.5R+ mS+LP	0.20 (w/p)	8[e]	2%	13/0.20; S	164

(O)PC: (ordinary) Portland cement; (z)SF: (zirconium) silica fume; mS: micro silica; FA: fly ash; LP: limestone powder; w/b: water to binder weight ratio; w/c: water to cement weight ratio; w/p: water to powder weight ratio; dmax: maximum diameter of coarse aggregate; Vf: fibre content; lf fibre length; df:fibre diameter fcm,28d: mean compressive strength at 28 days; 1HE: simple hooked-end; 2HE: double hooked-end; S: straight; C: crimped ends; nature of coarse aggregate: ([a]) flint, ([b]) limestone, ([c]) basalt, ([d]) granite, ([e]) diabase

2 Experimental Programme

2.1 Design of Experiments Strategy

The experiments were planned according to a Central Composite Design (CCD), which consists of three distinct sets of experimental runs: factorial (Fi), central (Ci) and axial (CCi) [13]. This approach helps to avoid the trial and error method and as a result, reduces the time necessary to develop the mixture of desired properties by collecting and statistically analysing relevant data. Additionally, it allows identifying design variables that have the most significant influence on the response variables, as well as the interactions between them. This design of experiments (DoE) technique involves the following steps: (1) choosing the mix-design variables and response variables; (2) selecting design variables' ranges; (3) conducting experiments and collecting data; (4) statistical analysis of data and fitting the empirical model, by means of regression analysis; (5) optimizing mixture proportions. In this work, the research program was first conducted at the mortar level and then on the concrete level to minimize at the beginning the number of design variables and therefore to reduce the number of experiments required to create the empirical model. After choosing the optimum paste composition, resulting from the study at the mortar level, the research on the concrete level was conducted.

Regarding the mortar stage, four key design variables were chosen: water to powder volume ratio (V_w/V_p); water to cement weight ratio (w/c); superplasticizer to powder weight ratio (Sp/p) and silica fume to cement weight ratio (SF/c) and four response variables: slump flow diameter (Dflow), V-funnel flow time (Tfunnel), compressive strength after 28 (fc,28d) and 98 days (fc,98d). It must be noted that sand to mortar volume ratio (V_s/V_m) and fibre content (V_f) were set fixed and equal to 0.475 and 1.5%, respectively. For concrete level, two key design variables were selected: solid volume ($V_g/V_{g,lim}$), sand to mortar volume ratio (V_s/V_m) and four response variables: time necessary to reach a 500 mm diameter in the slump flow test (t_{500}), slump flow diameter (Dflow), compressive strength after 7 (fc,7d) and 98 days (fc,98d). The fibre content (V_f) was fixed and equals 1.0%. The main reason to incorporate the steel fibres at this stage of the study was to avoid brittle failures in compression and reduce the variability of test results. More information about the formulation of the mixtures can be found elsewhere [13]. The effect of design variables was established on five levels: - α, -1, 0, +1, + α. Table 2 characterizes the experimental plans used for both the mortar and concrete studies.

After collecting the experimental data, the commercial software Design-Expert was used to analyse the results for each response variable namely, to examine the summary data plots, to fit 2^{nd} order polynomial models using regression analysis and ANOVA, to validate the models by examining the residuals for trends, autocorrelation and outliers, as well as to interpret the obtained model graphically.

Table 2. Experimental plans characterization

	Materials	Type of plan	Design variables	[-α; +α]	Response variables
Mortar level	CEM I 42.5R	**2^4Fi+8CCi+6Ci**	V_w/V_p	[0.450; 0.650]	Dflow
	Limestone powder	α= 2.0	w/c	[0.250; 0.350]	Tfunnel
	Silica fume	n_c= 6	Sp/p	[1.5%; 2.5%]	fc,28d
	Superplasticizer	n_f= 16	SF/c	[7.5%; 17.5%]	fc,98d
	standard sand	n_a= 8			
	Fibres (9/0.175;S)				
	Tap water				
Concrete level	CEM I 42.5R	**2^2Fi+4CCi+4Ci**	$V_g/V_{g,lim}$	[0.440; 0.510]	t_{500}
	Limestone powder	α= 1.414	V_s/V_m	[0.365; 0.435]	Dflow
	Silica fume	n_c= 4			fc,7d
	Superplasticizer	n_f= 4			fc,98d
	Sand	n_a= 4			
	Coarse aggregate				
	Fibres (13/0.2;S)				
	Tap water				

2.2 Constituent Materials

In the study at mortar level, the following materials were used: Type I Portland cement (CEM I 42.5R); limestone powder Betocarb® HP-OU (LP); silica fume Elkem 940-U (SF); standard sand; superplasticizer Sika® ViscoCrete® 20HE (Sp); straight steel fibres (l_f = 9 mm and d_f = 0.175 mm, f_y = 2100 MPa) and tap water. The specific gravity of cement, LP and SF were 3.07, 2.68 and 2.40 g/cm^3, respectively. The standard sand is siliceous natural sand with particles of diameter from 0.08 mm to 2 mm and round shape. Furthermore, specific gravity equals 2.63 g/cm^3 and water absorption 0.3% by mass. Regarding superplasticizers, the supplier provided the following information: specific gravity of 1.08 g/cm^3 and solid content of 40%.

Concerning the study at the concrete level, the same type of cement, LP, SF, Sp and tap water were used. However, standard sand was replaced by real aggregates: natural sand with a specific gravity of 2.58 g/cm^3 and water absorption of 0.7%; and a crushed coarse aggregate (d_{max} = 8 mm; amphibolite rock) whose specific gravity equals 3.02 g/cm^3 and water absorption is 0.6%. All concrete mixtures incorporated 1% of steel fibres (l_f = 13 mm and d_f = 0.2 mm, f_y = 2500 MPa), by volume.

2.3 Mixing Sequence and Testing Methods

Mortar mixes were tested in 1.40L batches at the low speed. The mixing procedure is presented in Table 3. To characterize the fresh state properties of mortar mixes (viscosity and flowability) the V- funnel and slump flow tests were carried out, respectively, according to Okamura & Ouchi proposal [14]. Firstly, the V-funnel was filled and the time that mortar needed to pass through the funnel opening was measured. Secondly, the slump flow test was conducted. At the beginning, the cone was filled and lifted with a constant speed. Then, after the flow of the mixture stopped, two diameters in perpendicular directions were measured. The final result (Dflow) is an average of four diameters because the test was repeated two times. Finally, four prisms of dimensions 40 × 40 × 160 mm^3 were cast to evaluate the compressive strength after 28 and 98 days. All the samples were covered with a plastic sheet to avoid drying and water evaporation. After 24 h, specimens were demoulded and placed underwater in a climatic chamber at 20 ± 2 °C, until the testing date. In the meantime, after 7 days, all the prism samples were cut into cubes of dimensions 40 × 40 × 40 mm^3. As a result, 12 samples for each mixture were obtained: 6 for testing the compressive strength after 28 days and 6 after 98 days. Afterwards, the average of these measures was calculated: fc,28d and fc,98d.

Table 3. Mortar mixing sequence

Task	Duration
Add sand + cement + limestone powder + silica fume + 80% of total mixing water	2.5min+ * +2.5min
Add 75% of superplasticizer + 20% of total mixing water	2.5min + *
Add 25% of superplasticizer	1.5min
Add fibers	2.0min+ * +1.0min
* Stop to scrape off the material adhering to the mixing walls	

Concrete mixes were tested in 25L batches in an open pan mixer. Steps of mixing procedure are presented in Table 4. The slump flow test was carried out according to EN 12350-8. When the cone was withdrawn upwards, the time from commencing the upward movement of the cone to when the concrete had flowed to a diameter of 500 mm was measured (t_{500}). Then, after the flow of the mixture stopped, two diameters in perpendicular directions were measured and their average was calculated (Dflow). Finally, six cubes of dimensions 150 × 150 × 150 mm^3 were cast to evaluate the compressive strength after 7 and 98 days. All the samples were covered with a plastic sheet to avoid drying and water evaporation. After 24 h, the specimens were demoulded and placed underwater and kept at 20 ± 2 °C until the testing age. Three samples were used to obtain compressive strength after 7 days and three after 98 days. Afterwards, the average of these measures was calculated: fc,7d and fc,98d.

Table 4. Concrete mixing sequence

Task	Duration
Add sand + 25% of total mixing water + coarse aggregate	2.5min
Waiting for absorption	2.5min
Add cement + limestone powder + silica fume + 75% of total mixing water + superplasticizer	5.0min + *
Add fibers	3.0min
* Stop to scrape off the material adhering to the mixing walls	

3 Experimental Campaign at Mortar Level

3.1 Collected Experimental Data

In this section, the results from tests carried out on mortar level are presented and discussed. Figure 2.a shows the range of results obtained in the fresh state. In general, the mortars exhibited very good flowability (Dflow $\geq$ 293 mm) and relatively high flow times, which indicates a low risk of segregation. In Fig. 2.b it can be seen that almost all mixtures experienced an increase of compressive strength from 28 to 98 days, ranging from 1.0% to 8.1%. For one mixture, the compressive strength decreased by about 1.1%. This can be a result of local defects of the tested samples.

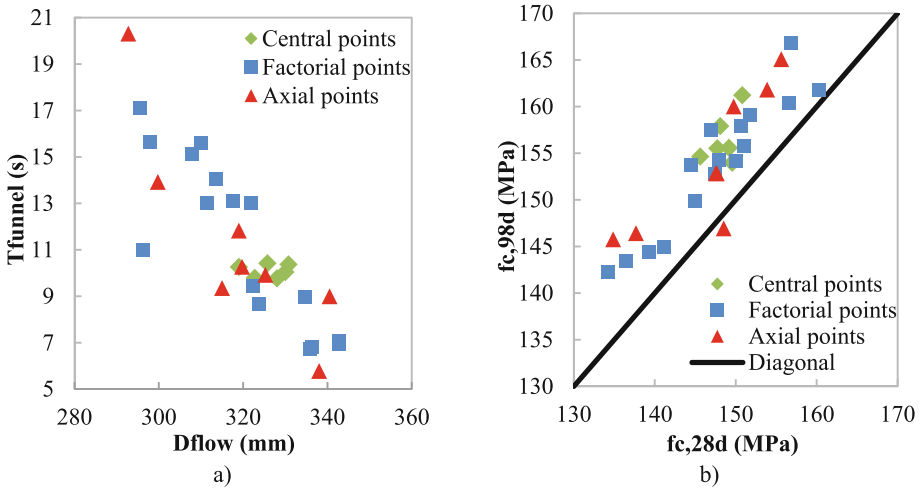

Fig. 2. Mortar test results: a) Tfunnel .vs. Dflow b) fc,98d.vs. fc,28d

3.2 Statistical Analysis of Data, Fitted Models and Optimisation

Table 5 presents the results of the fitted models, including the residual error term (ε), along with the correlation coefficients. An analysis of variance showed that these models are significant when describing the effect of Vw/Vp, w/c, Sp/p and SF/c on the

modelled responses. Since R^2 and R^2_{adj} values are significantly high, a large proportion of the variability of response variables is explained by the obtained regression models.

The estimates of the model coefficients presented in Table 5 indicate the relative significance of the various design variables on each response. Higher values indicate greater influence of the variable in the response and, on the other hand, a negative value reflects a response decrease to an increase in the design variable. Results in Table 5 clearly show Vw/Vp and w/c are the most influencing variables on the fresh state properties, while the compressive strength is influenced mainly by w/c and SF/c.

Based on the regression models presented in Table 5, the numerical optimization technique was used to determine the range of mortar mixture parameters that would lead to adequate self-compacting concrete (SCC) mixtures, with Tfunnel in between 12 and 14 s, a target compressive strength of 150 MPa and minimum cost of paste. No constraint was added concerning Dflow because all mixtures exhibited very good deformability. The selected optimised solution is presented in Table 6, in terms of the actual values. The optimised mortar mixture was also prepared and tested in the lab. The experimental results obtained compare well with the predicted values, which confirms the accuracy of the obtained fitted models.

Table 5. Fitted numerical models at mortar level (coded values of parameters)

	Dflow (mm)	Tfunnel (s)	fc,28d (MPa)	fc,98d (MPa)
Independent	322.931	9.993	147.534	155.585
Vw/Vp	**+11.439**	**-3.340**	-1.172	-1.594
w/c	**+7.915**	**-1.278**	**-5.486**	**-4.994**
Sp/p	*NS*	-0.367	*NS*	+0.558
SF/c	-3.019	+0.115	**+3.728**	**+3.715**
Vw/Vp×w/c	*NS*	*NS*	*NS*	+1.144
w/c×Sp/p	*NS*	+0.236	*NS*	-1.246
w/c×SF/c	*NS*	*NS*	*NS*	+1.225
Sp/p ×SF/c	*NS*	-0.251	*NS*	*NS*
$(Vw/Vp)^2$	-1.903	+0.764	*NS*	*NS*
$(w/c)^2$	*NS*	+0.367	*NS*	*NS*
$(Sp/p)^2$	*NS*	+0.264	*NS*	-1.582
*ε, std. dev.**	4.193	0.371	1.898	1.795
R^2 / R^2_{adj}	0.910 / 0.895	0.988 / 0.983	0.912 / 0.902	0.924/0.895

(NS) non-significant terms; (*) error term is a random and normally distributed variable with mean zero

Table 6. Optimised mortar mixture and corresponding predicted and measured test results

Design variables (actual values)		Dflow (mm)	Tfunnel (s)	fc,28d (MPa)
Vw/Vp=0.536	Measured	315.5	15.2	156.3
w/c=0.273	Predicted	314.0	14.0	150.0
Sp/p=1.59%	95% Prediction Interval- Low	304.0	12.8	145.6
SF/c=0.100	95% Prediction Interval-High	324.0	15.2	154.4
	Predicted/Measured	0.99	0.92	0.96

4 Experimental Campaign at Concrete Level

4.1 Collected Experimental Data

At the concrete level, concrete mixtures composition was obtained by considering the paste mixture proportions defined in Table 6 and replacing reference sand by real aggregates (fine and coarse aggregates described above). Tests on concrete are then necessary to optimize the aggregate skeleton and aggregates content. The DoE technique can also be applied at this stage to optimize concrete mixtures, considering as independent variables, only these variables related to the aggregates- Vg/Vg,lim and Vs/Vm- as detailed in Sect. 2.2.

The results from the tests carried at the concrete level are presented in Fig. 3. These results show that the designed experimental plan covers a wide range of Dflow (Fig. 3.a), including mixes that can be classified from SF1 to SF3 consistency classes. For all mixtures t_{500} is higher than 2 s, corresponding to VS2 class, according to EN 206-9. The relation between compressive strength after 7 days and slump flow diameter is plotted in Fig. 3.b. The range of fc,7d results obtained is very narrow (about 8 MPa), meaning that the changes introduced in the aggregate skeleton do not affect significantly the compressive strength. In Fig. 4 the slump flow of two extreme mixtures is presented. In the case of F4 mixture (the least fluid) slight aggregate segregation in the middle could be observed. On the other hand, with F1 mixture (the most fluid) separation of paste from aggregates took place at the edges. Also, the reduced workability of F4 led to a reduction in compressive strength (see Fig. 3.b), probably due to increased air content in the specimens.

4.2 Statistical Analysis of Data, Fitted Models and Optimisation

Table 7 presents the results of the fitted models for Dflow and t_{500} responses, including the residual error term (ε), along with the correlation coefficients. An analysis of variance showed that these models are significant when describing the effect of Vg/Vg, lim and Vs/Vm on the modelled responses. Since R^2 and R^2_{adj} values are significantly high, a large proportion of the variability of response variables is explained by the obtained regression models. As could be expected, both design variables - Vg/Vg,lim and Vs/Vm- influence significantly the analysed fresh state properties of SCC; Vs/Vm being the most influencing parameter. An increase of Vs/Vm or Vg/Vg,lim decreases the flowability and decreases the viscosity of the mixture (lower t_{500}).

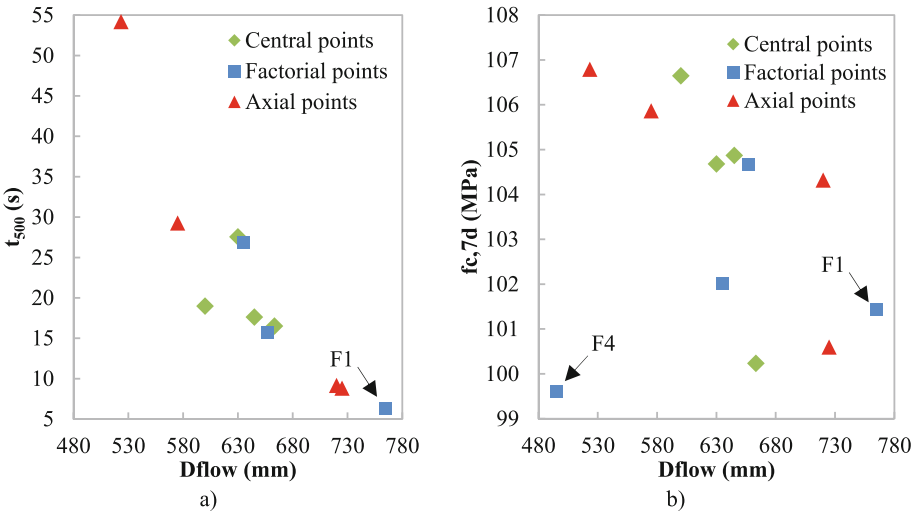

Fig. 3. Concrete test results: a) t_{500} .vs. Dflow; b) fc,7d .vs. Dflow

Fig. 4. Spread flow area of tested concrete mixtures: a) F4; b) F1

Again, the fitted numerical models and numerical optimization technique were used to determine the range of design variables that would lead to an SCC belonging to SF1 + VS2 consistency classes, while minimizing the volume of paste (or maximizing the total aggregates content). The best solution found corresponds to: Vg/Vg,lim = 0.453 and Vs/Vm = 0.430. The estimated response values of this mixture are: Dflow = 600 mm; t_{500} = 29.8 s; fc,7d ≈ 104 MPa (the average compressive strength of tested mixtures). In the next stage of this study, the benefits of hybridization (considering fibres with lengths of 13, 35 and 60 mm) on flexural strength will be assessed, in order to achieve the highest performance while keeping a relatively low fibre content.

Table 7. Fitted numerical models at concrete level (coded values of parameters)

	Dflow (mm)	$(1/t_{500}{}^{0.5})$ (s)
Independent	636.181	0.2315
Vg/Vg,lim	-57.454	-0.0634
Vs/Vm	**-71.329**	**-0.0858**
*ε, std. dev.**	17.650	0.026
R^2 / R^2_{adj}	0.951 / 0.941	0.927 / 0.911
(*) error term is a random and normally distributed variable with mean zero		

5 Conclusions

Most relevant conclusions of the current study are the following:

- The paste and aggregate particle phases and fibres mixture of HPFRC can be adjusted separately using DoE approach, allowing for mix-design optimisation.
- Fitted numerical models revealed that the workability and compressive strength of HPFRC mortars are mainly determined by the following pairs of design variables: (Vw/Vp, w/c) and (w/c, SF/C), respectively
- Total aggregates content was maximized to achieve an HPFRC exhibiting self-compacting ability (SF1 + VS2) while incorporating 1% straight steel fibres (l_f = 13 mm; d_f = 0.2 mm).

Acknowledgements. This work was financially supported by: UID/ECI/04708/2019- CONSTRUCT - Instituto de I&D em Estruturas e Construções and the project PTDC/ECI-EST/30511/2017 funded by national funds through the FCT/MCTES (PIDDAC). Collaboration and materials supply by EUROMODAL, Secil, Omya Comital, Sika, Krampharex and Dramix and is gratefully acknowledged.

References

1. Abbass, W., Khan, M.I., Mourad, S.: Evaluation of mechanical properties of steel fiber reinforced concrete with different strengths of concrete. Constr. Build. Mater. **168**, 556–569 (2018)
2. Okeh, C.A.O., Begg, D.W., Barnett, S.J., Nanos, N.: Behaviour of hybrid steel fibre reinforced self compacting concrete using innovative hooked-end steel fibres under tensile stress. Constr. Build. Mater. **202**, 753–761 (2019)
3. Jang, S.J., Jeong, G.Y., Yun, H.D.: Use of steel fibers as transverse reinforcement in diagonally reinforced coupling beams with normal- and high-strength concrete. Constr. Build. Mater. **187**, 1020–1030 (2018)
4. Ruano, G., Isla, F., Pedraza, R.I., Sfer, D., Luccioni, B.: Shear retrofitting of reinforced concrete beams with steel fiber reinforced concrete. Constr. Build. Mater. **54**, 646–658 (2014)

5. Mousavi, S.M., Ranjbar, M.M., Madandoust, R.: Combined effects of steel fibers and water to cementitious materials ratio on the fracture behavior and brittleness of high strength concrete. Eng. Fract. Mech. **216**(June), 106517 (2019)
6. Gholampour, A., Ozbakkaloglu, T.: Fiber-reinforced concrete containing ultra high-strength micro steel fibers under active confinement. Constr. Build. Mater. **187**, 299–306 (2018)
7. Deeb, R., Karihaloo, B.L., Kulasegaram, S.: Reorientation of short steel fibres during the flow of self-compacting concrete mix and determination of the fibre orientation factor. Cem. Concr. Res. **56**, 112–120 (2014)
8. Yoo, D.Y., Shin, H.O.: Bond performance of steel rebar embedded in 80–180 MPa ultra-high-strength concrete. Cem. Concr. Compos. **93**(February), 206–217 (2018)
9. Kazemi, M.T., Golsorkhtabar, H., Beygi, M.H.A., Gholamitabar, M.: Fracture properties of steel fiber reinforced high strength concrete using work of fracture and size effect methods. Constr. Build. Mater. **142**, 482–489 (2017)
10. Skazlic, M., Serdar, M., Bjegovic, D.: Influence of test specimens geometry on compressive performance concrete. In: Second International Symposium on Ultra High Performance Concrete (2008)
11. Piérard, J., Dooms, B., Cauberg, N.: Durability evaluation of different types of UHPC. In: RILEM-fib-AFGC Int. Symp. Ultra-High Perform. Fibre-Reinforced Concr. UHPFRC 2013 –, no. 1, pp. 275–284 (2013)
12. Li, P.P., Yu, Q.L., Brouwers, H.J.H.: Effect of coarse basalt aggregates on the properties of Ultra-high Performance Concrete (UHPC). Constr. Build. Mater. **170**, 649–659 (2018)
13. Nunes, S.: Performance-based design of self-compacting concrete (SCC): a contribution to enchance SCC mixtures robustness, p. 357 (2008)
14. Okamura, H., Ouchi, M.: Self-compacting concrete. Adv. Concr. Technol. **1**(1), 5–15 (2003)